島根大学地球資源環境学研究報告　33, 9～18 ページ（2015 年 2 月）
Geoscience Rept. Shimane Univ., 33, p.9～18（2015）

Article

Two modes of occurrence of garnets from the Tonaru metagabbro mass in the Sambagawa metamorphic belt, central Shikoku, Japan

Itsuki Kuraya*, Akira Takasu* and Md. Fazle Kabir*

Abstract

Garnet epidote amphibolite from the central part of the Tonaru metagabbro mass consists mainly of garnet, epidote and amphibole (ferro-hornblende), with small amounts of quartz, plagioclase (albite and oligoclase) and paragonite. Rutile, apatite, hematite, calcite and chlorite occur occasionally. Garnets in the garnet epidote amphibolites exhibit two modes of occurrence. Garnet 1 (Grt 1) occurs as porphyroblast, and garnet 2 (Grt 2) is found as fine grain in the matrix. Porphyroblastic garnets show a prograde growth zoning with increasing X_{Prp} and decreasing X_{Sps} from core to rim. Some of them display thin (<0.2 mm) outermost rim, which can be identify only from backscattered electron image. The outermost rim also shows a prograde growth zoning with outward decrease and increase in X_{Prp} and antithetic zoning in X_{Sps}. This outermost rim of porphyroblastic garnet (Grt 1) is similar to that of fine grained garnet (Grt 2). Diversity of the mode of occurrence and the chemical compositions of the garnets, the metamorphic evolution of the garnet epidote amphibolite is divided into two metamorphic events. These are a first high-pressure metamorphic event of eclogite facies (i) represented by porphyroblastic the garnet. And a second high-pressure which are metamorphic event (ii) is recorded by the outermost rim of porphyroblastic garnet and fine-grained garnet in the matrix, similar the prograde Sambagawa metamorphism of the oligoclase-biotite zone.

Key words: Sambagawa, porphyroblastic garnet, Tonaru metagabbro mass, garnet epidoteamphibolite

Introduction

The Sambagawa metamorphic belt is a Cretaceous high *P/T*-type metamorphic belt in Japan, and it extends from the Kanto Mountains, through Kii Peninsula and Shikoku to Kyushu for over 800 km with maximum width of 50 km in Shikoku (Fig. 1). The protoliths of the metamorphic rocks are dominated by sandstone and shale with small amounts of basalt, chert, and limestone. Metamorphic grade ranges from pumpellyite-actinolite facies through blueschist / greenschist facies to epidote-amphibolite facies, and locally to eclogite facies (e.g. Banno, 1964; Higashino, 1990; Enami *et al.*, 1994). In the Besshi district the metamorphic belt is divided into four zones based on index minerals in pelitic schists (Enami, 1983; Higashino, 1990). These are chlorite (300-360˚C, 5.5-6.5 kbar), garnet (425-470˚C, 7-8.5 kbar), albite-biotite (470-590˚C, 8-9.5 kbar) and oligoclase-biotite (585-635˚C, 9-11 kbar) zones (e.g. Enami, 1983; Higashino, 1990; Enami *et al.*, 1994). The mineral assemblages of the albite-biotite and oligoclase-biotite zones roughly coincide with those of epidote-amphibolite facies conditions, and their equilibrium *P-T* conditions have been estimated to be 8-11 kbar and 470-635˚C (Enami *et al.*, 1994). Several eclogite-bearing bodies occur throughout the albite-biotite and the oligoclase-biotite zones in the high-grade portions of the metamorphic sequence in the Besshi district, such as the Higashi-akaishi and Nikubuchi peridotite bodies, the Western Iratsu, Quartz Eclogite, Seba eclogitic basic schists, and the Sebadani, Eastern Iratsu and Tonaru metagabbro masses (e.g. Yokoyama, 1980; Takasu, 1984; Kunugiza *et al.*, 1986; Takasu, 1989; Aoya, 2001; Kugimiya and Takasu, 2002; Ota *et al.*, 2004; Miyagi and Takasu, 2005; Kabir and Takasu, 2010a, b; Endo and Tsuboi, 2013) (Fig. 1).

The Tonaru metagabbro mass is approximately 6.5 km× 1 km, and it is one of the eclogite-bearing bodies located in the central part of the Besshi district, which lies within the highest grade oligoclase-biotite zone of the Sambagawa sequence (Higashino, 1990) (Fig. 1). Compositional banding that reflects the original layered structure is widely developed in the mass, with schistosity defined by epidote-amphibolite facies minerals. The Tonaru metagabbro mass is considered to have been derived from a layered gabbro (Banno *et al.*, 1976; Kunugiza *et al.*, 1986; Takasu, 1989). The Tonaru mass occurs as a large lenticular body consisting two lithologies, the first is diopside amphibolite (T-I type amphibolite) with small amounts of serpentinite, and the second, garnet epidote amphibolite (T-II type amphibolite) accompanied by small amounts of eclogite (Moriyama, 1990) (Fig. 2). Kunugiza (1984) suggested that serpentinites within the diopside amphibolites were originally peridotites that were serpentinized, followed by subsequent prograde metamorphism. Takasu *et al.* (1994) suggested that the eclogite-bearing garnet epidote amphibolites underwent eclogite facies metamorphism before being retrograded into the epidote-amphibolite facies.

A detailed petrology and a metamorphic history of the Tonaru metagabbro mass have been reported by Miyagi and

*Department of Geoscience, Graduate School of Science and Engineering, Shimane University, 1060 Nishikawatsu, Matsue 690-8504, Japan

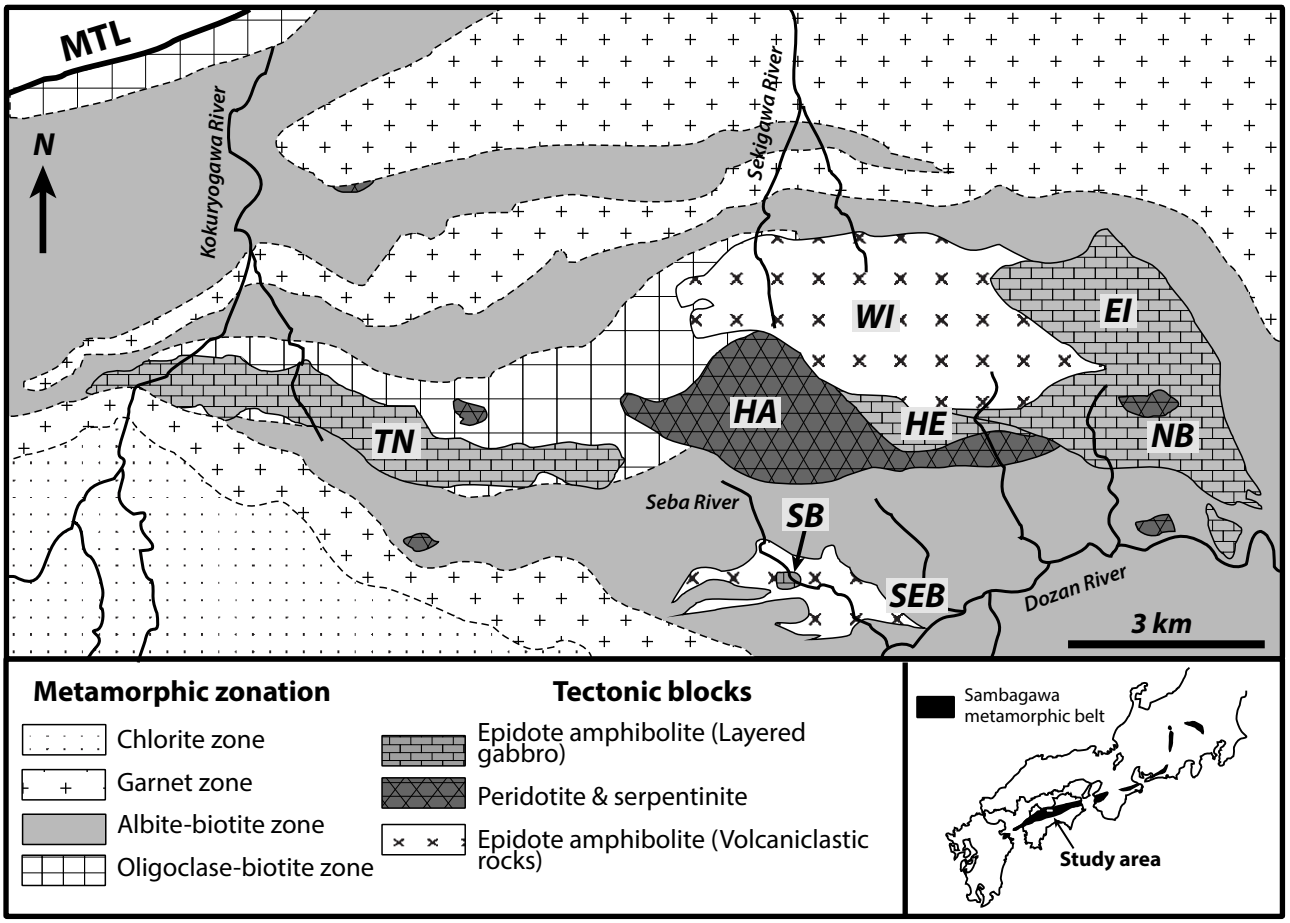

Fig. 1. Geological and metamorphic zonation map of the Sambagawa metamorphic belt in the Besshi district, central Shikoku, Japan (compiled from Takasu and Makino, 1980; Takasu, 1989; Higashino, 1990; Kugimiya and Takasu, 2002; Sakurai and Takasu, 2009; Kabir and Takasu, 2010a). SB, Sebadani metagabbro mass; SEB, Seba eclogitic basic schist; TN, Tonaru metagabbro mass; WI, Western Iratsu mass; EI, Eastern Iratsu mass; HA, Higashi-akaishi peridotite mass; HE, Hornblende eclogite mass; NB, Nikubuchi peridotite mass; MTL, Median Tectonic Line. Location for Figure 2 is also shown.

Takasu (2005). They suggested that the Tonaru metagabbro mass underwent three metamorphic events. A precursor metamorphic event (high-*T* amphibolite facies) that occurred before the prograde eclogite facies metamorphism is characterized by pargasite-taramite inclusions in the low-Ca inner cores of porphyroblastic garnets and Mg-rich relict cores of garnet (MgO ~ 8 wt%). The first high-*P* metamorphic event of the eclogite facies through the epidote-blueschist facies (300-450˚C and 7-11 kbar) to the eclogite facies (700-730˚C and ≥ 15 kbar), and subsequent retrogression into epidote-amphibolite facies. The eclogites were subsequently underwent another prograde metamorphism together with the surrounding Sambagawa schists, reaching oligoclase-biotite zone metamorphic conditions.

In this study we describe the texture, mode of occurrence and chemistry of zoned garnets in the Tonaru metagabbro mass. The mineral abbreviations used in the text, tables, and figures follow Whitney and Evans (2010) except for ferro-hornblende (FHbl).

Petrography of the garnet epidote amphibolite

Garnet epidote amphibolite samples were collected along the Ashidanigawa river at the central part of the Tonaru metagabbro mass (Fig. 2). A representative sample (2KT9) was selected for detail petrography. The garnet epidote amphibolite consists mainly of garnet, epidote and amphibole (ferro-hornblende), with small amounts of quartz, plagioclase (albite and oligoclase) and paragonite. Rutile, apatite, hematite, calcite and chlorite are occasionally present as accessory minerals. Preferred orientation of amphibole, paragonite and epidote defines schistosity and mineral lineation (Fig. 3a).

Garnets in the garnet epidote amphibolite have two modes of occurrence. Garnet 1 (Grt 1) occurs as porphyroblast and garnet 2 (Grt 2) is found as fine grains in the matrix. Garnet porphyroblasts in the matrix (Grt 1) occur as euhedral to subhedral porphyroblastic grains up to 1 cm across, optically zoned from pale pink-colored cores to colorless rims. Garnets are mostly inclusion free; some of them contain inclusions of rutile, epidote and quartz. Porphyroblastic garnets are frequently fractured and fractures are filled by amphibole

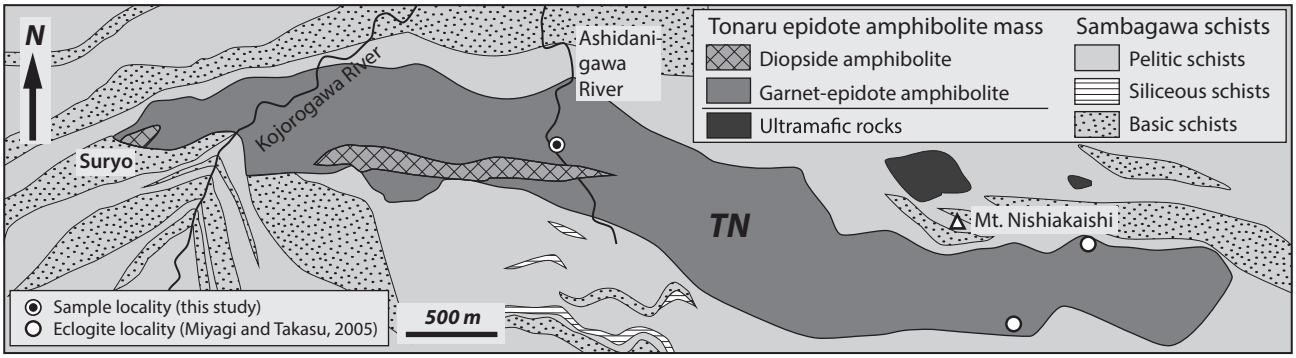

Fig. 2. Lithological map of the Tonaru metagabbro mass (after Miyagi and Takasu, 2005), with sample location (⊙). An eclogite locality of Miyagi and Takasu (2005) is also shown.

(FHbl), epidote, paragonite, chlorite and quartz. Some porphyroblastic garnets show thin (< 0.2 mm) outermost rim, which can be detected only from backscattered electron image by EPMA (Fig. 3b-c). Fine-grained garnets (Grt 2) found in the matrix occur as euhedral to subhedral grains up to 3 mm across (Fig. 3d). They mostly lack inclusions. These garnets are sometimes fractured and fractures are filled by amphibole (FHbl), chlorite and quartz.

Chemical compositions of the garnets

Chemical composition and compositional zoning of the garnets in the Seba pelitic schists were investigated in Shimane University, using JEOL JXA 8800M and 8530F electron microprobe analyzers. Analytical conditions used for quantitative analysis were 15 kV accelerating voltage, 20 nA specimen current, and 5 μm beam diameter. Correction procedure was carried out as described by Bence and Albee (1968). Ferric iron contents in garnet were estimated using charge balance $Fe^{3+} = 8\text{-}2Si\text{-}2Ti\text{-}Al$ (O = 12). Na (< 0.10 wt%), K (< 0.07 wt%) and Cr (< 0.06 wt%) contents are negligible.

The porphyroblastic garnets (Grt 1) have almandine-rich composition (X_{Alm} 0.54-0.63), with variable amounts of the grossular (X_{Grs} 0.16-0.24), spessartine (X_{Sps} 0-0.08) and pyrope (X_{Prp} 0.13-0.23) components. Two zones (core and rim) were identified based on chemical composition (Table 1; Figs. 3a-b, 4 and 5). The garnets show a growth zoning, with X_{Sps} decreasing gently from the inner core to the outer core (0.08-0.07), and sharply decreasing toward the rim (0.07-0) (Figs. 4a, 5a-b). Slight increasing X_{Alm} from inner core to the outer core and decrease towards the rims (0.58-0.60-0.54). X_{Grs} increases from the inner core to the middle core (0.18-0.19), although with some fluctuation, and then decreases and increase to the rim (0.19-0.17-0.24). Pyrope contents increase gently from inner core to outer core (X_{Prp} 0.13-0.20), slightly decrease and increase (X_{Prp} 0.20-0.18-0.21) from outer core to the rim.

Some porphyroblastic garnets display thin outermost rim, in which, X_{Grs} (0.20-0.30-0.29) and X_{Sps} (0.04-0.06-0.01) increase and slight decrease from rim to outermost rim and X_{Prp} showing antithetic zoning (0.21-0.19-0.22). X_{Alm} increases from the rim and decreases towards the outermost rim (0.54-0.58-0.47) (Figs. 4b, 5a-b).

Fine-grained garnets show homogeneous in the core. Rim of the garnets shows a zoning, with increasing and slight decreasing X_{Sps} (0.03-0.06-0.05) and opposite zoning of X_{Prp} (0.19-0.16-0.17) from core to rim (Fig. 4c). The compositional zoning of the fine-grained garnets (Grt 2) is similar to that of the outermost rims of porphyroblastic garnet (Grt 1).

The chemical compositions of fine-grained garnets are fairly homogeneous, and X_{Mg} slightly increases toward the rim (0.23-0.30). The compositions are similar to those of the rims of the porphyroblastic garnets. Mg-rich fragmented porphyroblastic garnets in the garnetepidote amphibolites show Mg-rich composition, and zoning with resorbed core (X_{Mg} 0.40) and Mg-poor (X_{Mg} 0.20) and Mn-rich rim.

Discussion and Conclusions

Two modes of occurrence and wide range of chemical compositions of the garnets (Grt 1-2) in the Tonaru garnet epidote amphibolite provide important information on the Sambagawa metamorphism and suggest a variety of equilibrium metamorphic *P-T* conditions.

Miyagi and Takasu (2005) reported three modes of occurrence of garnet in the garnet epidoteamphibolite, i.e. porphyroblastic garnet, fine-grained garnet, and high-Mg fragmental garnet. Porphyroblastic garnets are almandine-rich, and X_{Prp} (0.16-0.23) and X_{Grs} (0.20-0.30) increase from core to rim (Fig. 5a-b). Matsuura *et al.* (2013) also reported porphyroblastic garnet from kyanite-free garnet amphibolite from the western part of the Tonaru metagabbro mass. Porphyroblastic garnets are almandine-rich in composition and nearly homogeneous X_{Prp} (0.15-0.18) and X_{Grs} (0.13-0.18) (Fig. 5a-b).

The porphyroblastic garnets (Grt 1) in the present study also have almandine-rich composition, with variable amounts of the grossular (X_{Grs} 0.16-0.24), and pyrope (X_{Prp} 0.13-0.23). The chemical compositions of the porphyroblastic

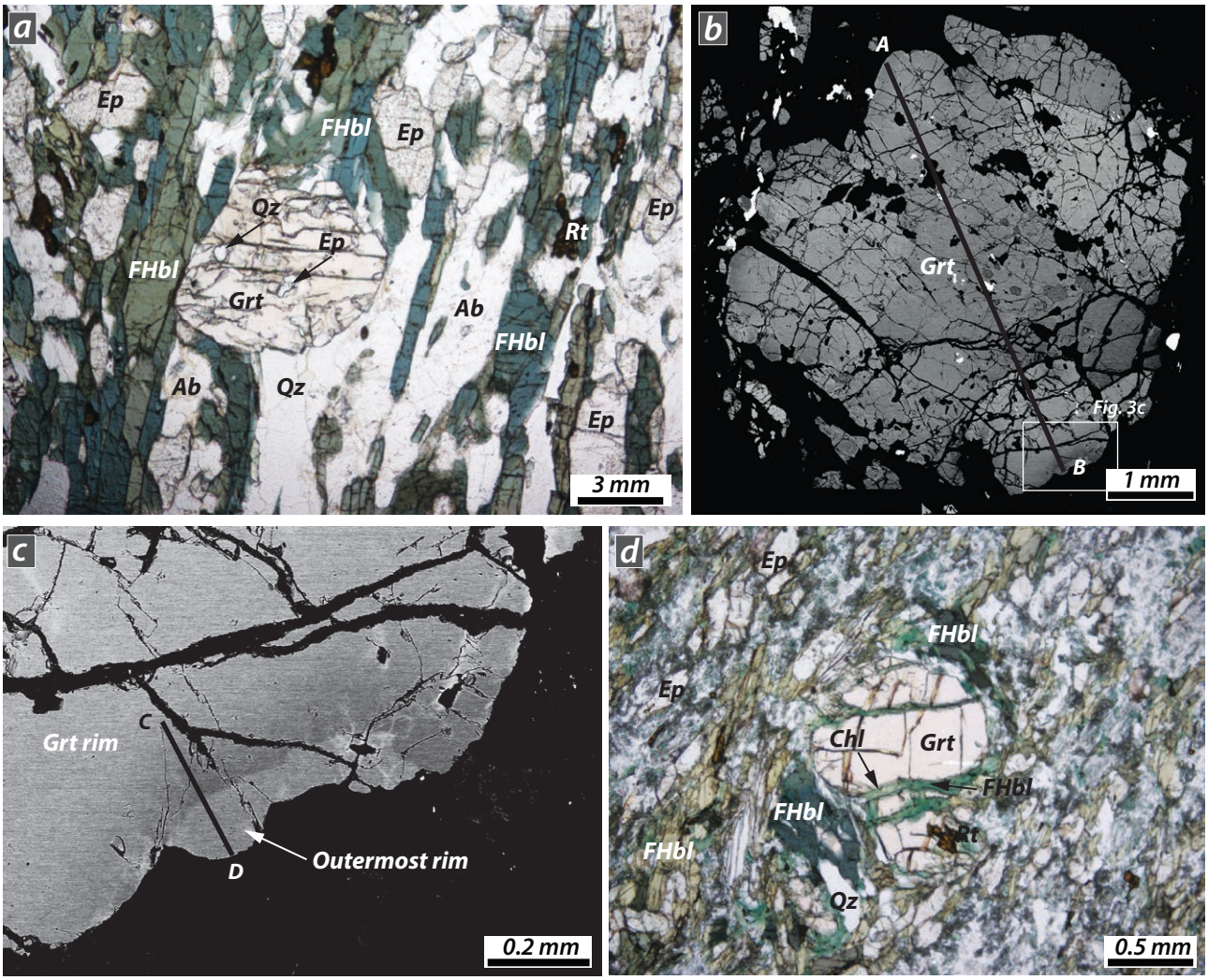

Fig. 3. Photomicrographs and backscattered electron images showing textural relationships of minerals in the Tonaru garnet epidote amphibolites. (a) Porphyroblastic garnet (Grt 1) and the other matrix minerals of amphibole (FHbl), epidote, albite, rutile and quartz. (b) Porphyroblastic garnet (Grt 1) showing relatively dark core and light rim. (c) Outermost rim of the porphyroblastic garnet is identified by backscattered electron image. (d) Fine-grained garnet and the other matrix minerals of epidote, amphibole (FHbl) and quartz. Garnet fractures are filled by ferro-hornblende and chlorite.

garnets are similar to those described by Miyagi and Takasu (2005) and Matsuura *et al.* (2013). Only Miyagi and Takasu (2005) reported slightly higher in X_{Prp} and X_{Grs} at their rim. Porphyroblastic garnets in the present study show a prograde growth zoning with increasing X_{Prp} (0.13-0.21) and decreasing X_{Sps} (0.08-0) from core to rim. Some porphyroblastic garnets in the garnet epidote amphibolite display thin (< 0.2 mm) outermost rim, which can be identify only from backscattered electron image. This outermost rim also shows a prograde growth zoning with outward decrease and increase in X_{Prp} (0.21-0.19-0.22) and antithetic zoning in X_{Sps} (0.04-0.06-0.01) (Fig. 4b). This outer most rim of porphyroblastic garnet (Grt 1) is similar to that of fine grained garnet (Grt 2) in the matrix.

On the basis of petrography and the chemical composition of the garnets, the metamorphic evolution of the garnet epidote amphibolite from the central part of the Tonaru metagabbro mass can be divided into two metamorphic events. These are a first high-pressure metamorphic event (i) represented by porphyroblastic garnet, and a second high-pressure metamorphic event (ii) recorded by the outermost rim of porphyroblastic garnet and fine-grained garnet in the matrix. The porphyroblastic garnets in the garnet epidoteamphibolite formed in the prograde metamorphism of high-*P* metamorphic event; during the retrograde metamorphism the porphyroblastic garnets were fractured. Miyagi and Takasu (2005) reported a *P-T* path of eclogite and garnet epidoteamphibolite metamorphism. The prograde path passes through the epidote-blueschist facies to the eclogite facies peak at 700-730˚C and ≥ 15 kbar, followed by retrograde metamorphism into the epidote–amphibolite facies. The porphyroblastic garnet in the present study probably follow a similar prograde, peak and retrograde *P-T* path of the Tonaru eclogite and garnet epidoteamphibolite.

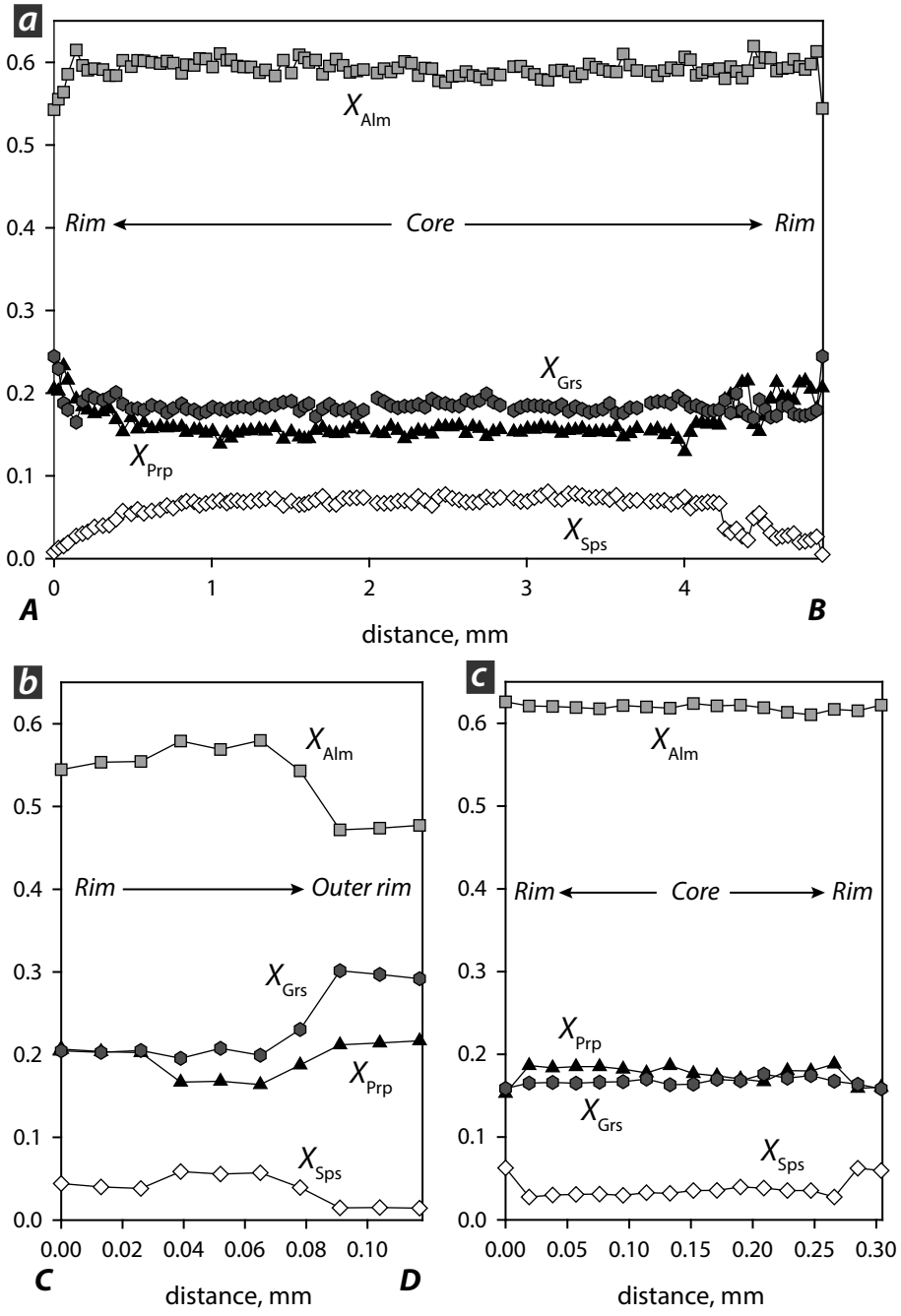

Fig. 4. Chemical compositions of zoned garnets from the Tonaru garnet epidote amphibolites. (a) Compositional profile of garnet (Grt 1) from the core to the rim in terms of X_{Alm}, X_{Prp}, X_{Grs} and X_{Sps} contents (from figure 3b). (b) Compositional profile of outermost rim of the garnet (Grt 1) (from figure 3c). (c) Compositional profile of Grt 2.

The outermost rim of the porphyroblastic garnets and the fine-grained garnets in the matrix are probably developed at the second high-*P* metamorphic event. This metamorphic event is maybe correlated to that of the prograde Sambagawa metamorphism of the oligoclase-biotite zone, as reported by Miyagi and Takasu, (2005).

Acknowledgements

We thank the members of the Geoscience and Metamorphic Geology Seminars of Shimane University for discussion and helpful suggestions, and Hiroaki Komuro for critical reading and comments on the manuscript. Thanks are also due to Yasunori Kondo for his support during fieldwork. This study was partly supported by JSPS KAKENHI Grant (No. 24340123) to A.T.

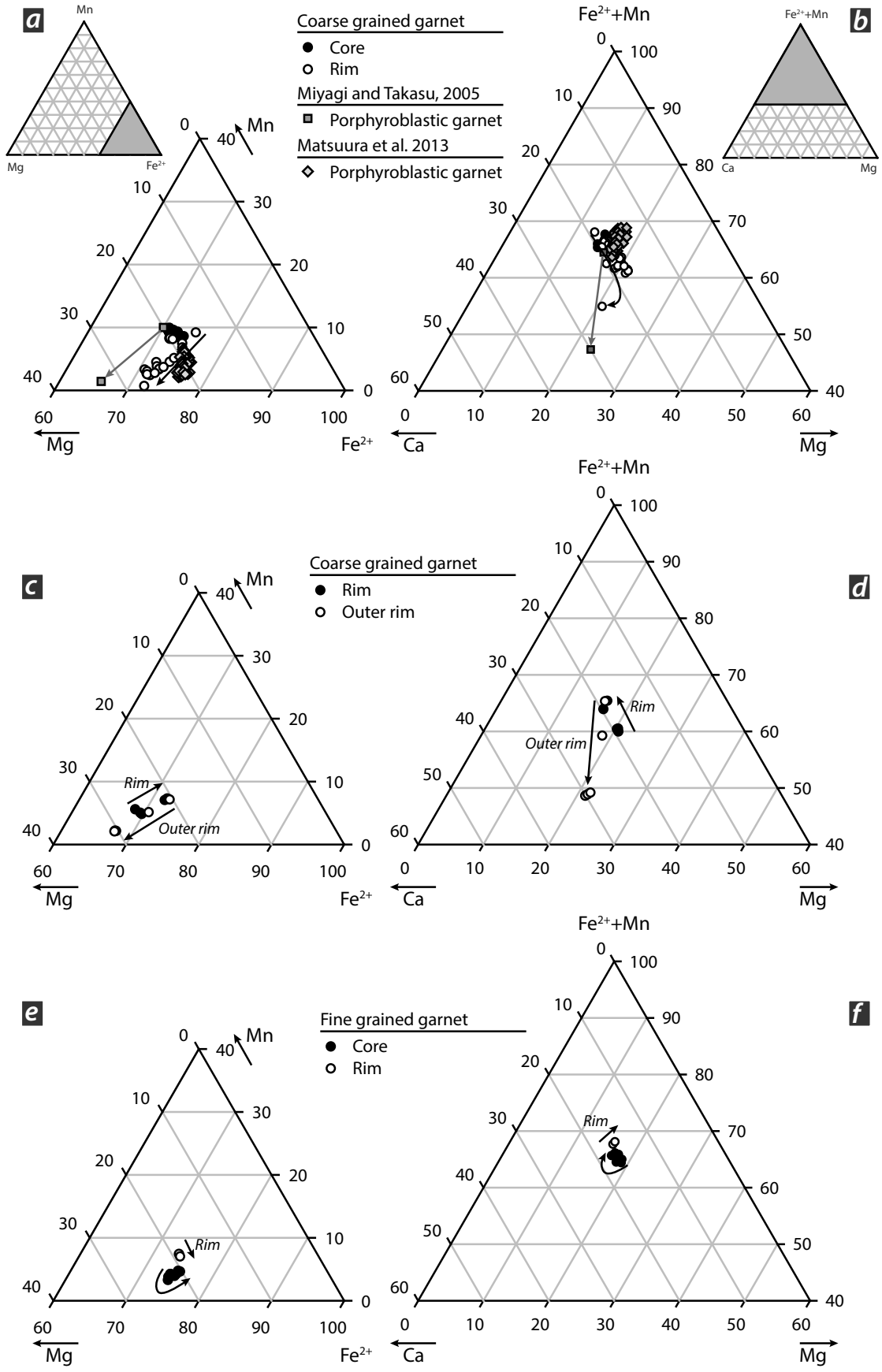

Fig. 5. (a-d) Composition of garnet (Grt 1) from the Tonaru garnet epidote amphibolites (this study) in terms of Fe^{2+}, Mn, Mg and Ca. Garnet compositions from the garnet epidote amphibolite of Miyagi and Takasu (2005) and Matsuura *et al.* (2013) are also shown. (e-f) Composition of fine-grained garnet (Grt 2)

Referrences

Aoya, M., 2001, *P-T-D* path of eclogite from the Sambagawa belt deduced from combination of petrological and microstructural analyses. *Journal of Petrology*, **42**, 1225-1248.

Banno, S., 1964, Petrological studies of the Sanbagawa crystalline schists in the Bessi-Ino district, central Shikoku, Japan. *Journal of the Faculty of Science, Tokyo University, Section II*, **15**, 203-319.

Banno, S., Yokohama, K., Enami, M., Iwata, O., Nakamura, K. and Kasashima, S., 1976, Petrography of the peridotite-metagabbro complex in the vicinity of Mt. Higashi-akaishi, Central Shikoku. Part I. Megascopic textures of the Iratsu and Tonaru epidote amphibolite masses. *The Science Reports of Kanazawa University*, **21**, 139-159.

Bence, A. E. and Albee, A. L., 1968, Empirical correction factors for the electron microanalysis of silicates and oxides. *Journal of Geology*, **76**, 382-403.

Enami, M., 1983, Petrology of pelitic schists in the oligoclase-biotite zone of the Sanbagawa metamorphic terrain, Japan: phase equilibria in the highest grade zone of a high-pressure intermediate type of metamorphic belt. *Journal of Metamorphic Geology*, **1**, 141-161.

Enami, M., Wallis, S. R. and Banno, Y., 1994, Paragenesis of sodic pyroxene-bearing quartz schists: implications for the *P-T* history of the Sanbagawa belt. *Contributions to Mineralogy and Petrology*, **116**, 182-198.

Endo, S. and Tsuboi, M., 2013, Petrogenesis and implications of jadeite-bearing kyanite eclogite from the Sanbagawa belt (SW Japan). *Journal of Metamorphic Geology*, **31**, 647-661.

Higashino, T., 1990, The higher grade metamorphic zonation of the Sambagawa metamorphic belt in central Shikoku, Japan. *Journal of Metamorphic Geology*, **8**, 413-423.

Kabir, M. F. and Takasu, A., 2010a, Evidence for multiple burial–partial exhumation cycles from the Onodani eclogites in the Sambagawa metamorphic belt, central Shikoku, Japan. *Journal of Metamorphic Geology*, **28**, 873-893.

Kabir, M. F. and Takasu, A., 2010b, Glaucophanic amphibole in the Seba eclogitic basic schists, Sambagawa metamorphic belt, central Shikoku, Japan: implications for timing of juxtaposition of the eclogite body with the non-eclogite Sambagawa schists. *Earth Sciences*, **64**, 183-192.

Kugimiya, Y. and Takasu, A., 2002, Geology of the Western Iratsu mass within the tectonic melange zone in the Sambagawa metamorphic belt, Besshi district, central Shikoku, Japan. *Journal of the Geological Society of Japan*, **108**, 644-662.

Kunugiza, K., 1984, Metamorphism and origin of ultramafic bodies of the Sanbagawa Metamorphic Belt in central Shikoku. *Journal of the Japanese Association for Mineralogists, Petrologists and Economic Geologists*, **79**, 20-32.

Kunugiza, K., Takasu, A. and Banno, S., 1986, The origin and metamorphic history of the ultramafic and metagabbro bodies in the Sanbagawa Metamorphic Belt. *Geological Society of America Memoir*, **164**, 375-386.

Matsuura, H., Takasu, A. and Kabir, M. F., 2013, High–Mg garnets in kyanite garnet amphibolite from the Tonaru metagabbro mass in the Sambagawa metamorphic belt, Besshi district, central Shikoku, Japan. *Geoscience Reoprts of Shimane University, Japan*, **32**, 13-22.

Miyagi, Y. and Takasu, A., 2005, Prograde eclogites from the Tonaru epidote amphibolite mass in the Sambagawa Metamorphic Belt, central Shikoku, southwest Japan. *Island Arc*, **14**, 215-235.

Moriyama, H., 1990, Two metamorphic paths in the Tonaru epidote amphibolite mass within the Sambagawa belt, Besshi district, central Shikoku. *Geoscience Reports of Shimane University, Japan*, **9**, 49-54.

Ota, T., Terabayashi, M. and Katayama, I., 2004, Thermobaric structure and metamorphic evolution of the Iratsu eclogite body in the Sanbagawa belt, central Shikoku, Japan. *Lithos*, **73**, 95-126.

Sakurai, T. and Takasu, A., 2009, Geology and metamorphism of the Gazo mass (eclogite-bearing tectonic block) in the Sambagawa metamorphic belt, Besshi district, central Shikoku, Japan. *Journal of Geological Society of Japan*, **115**, 101-121.

Takasu, A., 1984, Prograde and retrograde eclogites in the Sambagawa metamorphic belt, Besshi district, Japan. *Journal of Petrology*, **25**, 619-643.

Takasu, A., 1989, *P-T* histories of peridotite and amphibolite tectonic blocks in the Sanbagawa metamorphic belt, Japan. In: *Evolution of Metamorphic Belts* (eds Daly, J. S., Cliff, R. A. & Yardley, B. W. D.), Geological Society, London, Special Publications. **43**, 533-538, Blackwell Scientific Publications, Oxford.

Takasu, A. and Makino, K., 1980, Stratigraphy and geologic structure of the Sanbagawa metamorphic belt in the Besshi district, Shikoku, Japan (Reexamination of the recumbent fold structures). *Earth Science*, **34**, 16-26 (in Japanese with English abstract).

Takasu, A., Wallis, S. R., Banno, S. and Dallmeyer, R. D., 1994, Evolution of the Sambagawa metamorphic belt, Japan. *Lithos*, **33**, 119-133.

Whitney, D. L. and Evans, B. W., 2010, Abbreviations for names of rock-forming minerals. *American Mineralogist*, **95**, 185-187.

Yokoyama, K., 1980, Nikubuchi peridotite body in the Sanbagawa metamorphic belt; thermal history of the 'Al-pyroxene-rich suite'peridotite body in high pressure metamorphic terrain. *Contributions to Mineralogy and Petrology*, **73**, 1-13.

(Received: Oct. 10, 2014, Accepted: Jan. 16, 2015)

（要　旨）

蔵谷　樹・高須　晃・Md. Fazle Kabir, 2014 四国中央部別子地域三波川変成帯の東平変斑れい岩体中の二種のざくろ石．島根大学地球資源環境学研究報告，33, 9-18.

東平変斑れい岩体は三波川変成帯中の高度変成岩体の一つとして産する．岩体は少量の蛇紋岩を伴う透輝石角閃岩と少量のエクロジャイトを伴うざくろ石緑れん石角閃岩からなる．東平岩体中央部に産するざくろ石緑れん石角閃岩は角閃石（フェロホルンブレンド），ざくろ石，緑れん石，パラゴナイト，緑泥石，石英，赤鉄鉱からなる．これらは角閃石に富む層と斜長石に富む層の互層からなる層状構造を示す．ざくろ石緑れん石角閃岩中のざくろ石には斑晶変晶のもの（Grt 1）と直径 0.2 mm 以下（Grt 2）の細粒のものの二種類が存在する．この二種類のどちらの最外縁部にも昇温で成長したと考えられる部分があり，X_{Prp}（0.21-0.19-0.22）は減少した後に増加し，X_{Sps}（0.04-0.06-0.01）はそれに反比例する．ざくろ石の化学組成からざくろ石緑れん石角閃岩は二回の変成イベントを経ているとした．エクロジャイト相での高圧変成作用（i）はざくろ石斑晶変晶の存在から定義される．二度目の高圧変成イベント（ii）は二種類のざくろ石にみられる最外縁部から定義される．この二度目の変成イベントはオリゴクレース - 黒雲母帯の三波川昇温変成ステージに対比できる可能性がある。

Table 1. Representative chemical compositions of garnets from the Tonaru garnet epidote amphibolites.

Sample	2KT9																			
Analysis	68	69	70	71	72	73	74	75	76	77	78	82	85	86	87	88	89	90	91
Mode	Grt 1	Grt 1	Grt 1	Grt 1	Grt 1	Grt 1	Grt 1	Grt 1	Grt 1	Grt 1	Grt 1	Grt 1	Grt 1	Grt 1	Grt 1	Grt 1	Grt 1	Grt 1	Grt 1
	Rim	←	←	←	←	←	←	←	←	←	←	←	←	←	←	←	←	←	←
SiO_2	39.25	39.19	39.24	39.20	38.44	38.49	38.78	38.66	38.92	38.95	38.85	38.67	38.54	38.48	38.53	38.51	38.90	38.73	39.04
TiO_2	0.06	0.04	0.09	0.04	0.04	0.09	0.11	0.09	0.09	0.09	0.09	0.01	0.08	0.11	0.08	0.10	0.09	0.06	0.10
Al_2O_3	21.84	21.57	21.86	21.56	21.44	21.48	21.53	21.55	21.64	21.65	21.31	21.40	21.14	21.31	21.46	21.37	21.19	21.48	21.58
FeO*	24.27	25.18	25.24	26.03	27.65	26.47	26.35	26.41	26.66	26.66	25.90	26.39	26.45	26.58	26.82	26.77	26.42	26.42	27.02
MnO	0.35	0.57	0.67	0.82	1.22	1.32	1.42	1.69	1.77	1.82	2.08	2.49	2.38	2.60	2.41	2.54	2.57	2.78	2.72
MgO	5.14	5.15	5.85	5.38	4.87	4.57	4.50	4.38	4.49	4.63	4.18	3.77	4.25	3.88	4.10	3.93	3.95	3.89	4.02
CaO	8.53	8.12	6.56	6.24	5.79	6.59	6.89	6.75	6.74	6.94	6.94	6.39	6.28	6.25	6.24	6.45	6.31	6.05	6.39
Total	99.44	99.82	99.51	99.27	99.45	99.01	99.58	99.53	100.31	100.74	99.35	99.12	99.12	99.21	99.64	99.67	99.43	99.41	100.87
Cations on the basis of 12 oxygens																			
Si	3.07	3.06	3.06	3.08	3.03	3.05	3.65	3.05	3.05	3.02	3.07	3.08	3.06	3.06	3.05	3.05	3.08	3.07	3.05
Ti	0.00	0.00	0.01	0.00	0.00	0.01	0.01	0.01	0.00	0.01	0.01	0.00	0.01	0.01	0.01	0.01	0.01	0.00	0.01
Al	2.01	1.98	2.01	2.00	2.00	2.00	2.00	2.00	2.00	1.99	1.99	2.00	1.98	2.00	2.00	1.99	1.98	2.01	1.99
Fe*	1.59	1.64	1.65	1.71	1.83	1.75	1.74	1.74	1.75	1.74	1.71	1.76	1.76	1.77	1.77	1.77	1.75	1.75	1.77
Mn	0.02	0.04	0.04	0.05	0.08	0.09	0.10	0.10	0.12	0.12	0.14	0.17	0.16	0.17	0.16	0.17	0.17	0.19	0.18
Mg	0.60	0.60	0.68	0.63	0.57	0.54	0.52	0.52	0.52	0.54	0.49	0.45	0.50	0.46	0.49	0.46	0.47	0.46	0.47
Ca	0.71	0.68	0.55	0.53	0.49	0.56	0.58	0.57	0.57	0.58	0.59	0.54	0.53	0.53	0.53	0.55	0.54	0.52	0.53
Total	8.00	8.00	8.00	8.00	8.00	8.00	8.00	8.00	8.00	8.00	8.00	8.00	8.00	8.00	8.00	8.00	8.00	8.00	8.00
X_{Prp}	0.21	0.20	0.23	0.21	0.19	0.18	0.18	0.18	0.18	0.18	0.17	0.15	0.17	0.16	0.16	0.16	0.16	0.16	0.16
X_{alm}	0.54	0.56	0.56	0.59	0.62	0.60	0.59	0.59	0.59	0.58	0.58	0.60	0.60	0.60	0.60	0.60	0.60	0.60	0.60
X_{Grs}	0.24	0.23	0.19	0.18	0.16	0.19	0.20	0.19	0.19	0.20	0.20	0.19	0.18	0.18	0.18	0.18	0.18	0.18	0.18
X_{Sps}	0.01	0.01	0.02	0.02	0.03	0.03	0.03	0.04	0.04	0.04	0.05	0.06	0.05	0.06	0.06	0.06	0.06	0.06	0.06

**Total Fe as FeO*

Sample	2KT9																			
Analysis	94	95	96	97	98	99	100	101	102	103	104	105	106	107	108	109	110	111	112
Mode	Grt 1	Grt 1	Grt 1	Grt 1	Grt 1	Grt 1	Grt 1	Grt 1	Grt 1	Grt 1	Grt 1	Grt 1	Grt 1	Grt 1	Grt 1	Grt 1	Grt 1	Grt 1	Grt 1
	←	←	←	←	←	←	←	←	←	←	←	←	←	←	←	←	←	←	←
SiO_2	38.74	38.88	38.69	38.56	38.81	38.41	38.75	38.71	38.71	38.78	38.56	38.61	38.94	38.74	38.88	38.83	39.01	38.39	38.70
TiO_2	0.10	0.09	0.10	0.08	0.10	0.08	0.08	0.04	0.07	0.08	0.07	0.12	0.10	0.06	0.09	0.07	0.13	0.08	0.09
Al_2O_3	21.36	21.53	21.22	21.29	21.36	21.47	21.29	21.33	21.29	21.49	21.25	21.52	21.11	21.50	21.60	21.21	21.32	21.25	21.43
FeO*	26.16	27.12	27.19	26.79	26.86	26.08	27.28	27.23	27.07	26.78	26.21	26.54	25.89	26.32	25.93	27.05	26.05	27.30	27.06
MnO	2.95	3.11	3.09	2.82	2.93	2.98	3.10	3.00	3.09	3.11	2.96	3.06	3.06	3.18	3.18	2.84	3.05	2.88	2.90
MgO	3.98	3.89	3.98	3.86	3.78	3.78	3.47	3.85	3.67	3.83	3.81	3.87	3.86	3.85	3.95	3.64	3.81	3.70	3.63
CaO	6.51	6.42	6.40	6.08	6.16	6.27	6.31	6.30	6.36	6.42	6.32	6.34	6.40	6.36	6.44	6.62	6.59	6.26	6.43
Total	99.80	101.04	100.67	99.48	100.00	99.07	100.28	100.46	100.26	100.49	99.18	100.06	99.36	100.01	100.07	100.26	99.96	99.86	100.24
Cations on the basis of 12 oxygens																			
Si	3.06	3.04	3.04	3.06	3.07	3.06	3.06	3.05	3.05	3.05	3.07	3.05	3.09	3.06	3.06	3.06	3.08	3.04	3.05
Ti	0.01	0.01	0.01	0.00	0.01	0.00	0.01	0.00	0.00	0.00	0.00	0.01	0.01	0.00	0.01	0.00	0.01	0.00	0.01
Al	2.00	1.98	1.96	1.99	1.99	2.02	1.98	1.98	1.98	1.99	1.99	2.00	1.97	2.00	2.01	1.97	1.98	1.99	1.99
Fe*	1.73	1.77	1.78	1.78	1.77	1.74	1.80	1.79	1.79	1.76	1.75	1.75	1.72	1.74	1.71	1.79	1.72	1.81	1.78
Mn	0.20	0.21	0.20	0.19	0.19	0.20	0.21	0.20	0.21	0.21	0.20	0.20	0.21	0.21	0.21	0.19	0.20	0.19	0.20
Mg	0.47	0.45	0.47	0.46	0.45	0.45	0.41	0.45	0.43	0.45	0.45	0.45	0.46	0.45	0.46	0.43	0.45	0.44	0.43
Ca	0.55	0.54	0.54	0.52	0.52	0.53	0.53	0.53	0.54	0.54	0.54	0.54	0.54	0.54	0.54	0.56	0.56	0.53	0.54
Total	8.00	8.00	8.00	8.00	8.00	8.00	8.00	8.00	8.00	8.00	8.00	8.00	8.00	8.00	8.00	8.00	8.00	8.00	8.00
X_{Prp}	0.16	0.15	0.16	0.16	0.15	0.15	0.14	0.15	0.15	0.15	0.15	0.15	0.16	0.16	0.16	0.14	0.15	0.15	0.14
X_{alm}	0.59	0.60	0.60	0.60	0.60	0.60	0.61	0.60	0.60	0.60	0.59	0.60	0.59	0.59	0.58	0.60	0.59	0.61	0.61
X_{Grs}	0.19	0.18	0.18	0.18	0.18	0.18	0.18	0.18	0.18	0.18	0.18	0.18	0.18	0.18	0.19	0.19	0.19	0.18	0.18
X_{Sps}	0.06	0.07	0.07	0.06	0.07	0.07	0.07	0.07	0.07	0.07	0.07	0.07	0.07	0.07	0.07	0.07	0.07	0.06	0.07

**Total Fe as FeO*

Sample	2KT9																			
Analysis	113	114	115	116	117	118	119	120	120	123	124	125	126	127	128	129	130	131	132
Mode	Grt 1	Grt 1	Grt 1	Grt 1	Grt 1	Grt 1	Grt 1	Grt 1	Grt 1	Grt 1	Grt 1	Grt 1	Grt 1	Grt 1	Grt 1	Grt 1	Grt 1	Grt 1	Grt 1
	←	←	←	←	←	←	←	←	←	←	←	←	←	←	←	←	←	←	←
SiO_2	38.75	38.55	38.74	38.93	39.12	38.78	38.70	38.36	38.47	38.69	38.78	39.19	38.70	38.94	38.66	38.88	38.77	38.81	39.12
TiO_2	0.11	0.05	0.11	0.08	0.09	0.12	0.09	0.02	0.11	0.05	0.08	0.08	0.09	0.08	0.06	0.11	0.08	0.10	0.08
Al_2O_3	21.39	21.47	21.32	21.44	21.48	21.34	21.39	21.40	21.18	21.46	21.47	21.49	21.35	21.47	21.33	21.26	21.32	21.31	21.56
FeO*	26.51	27.37	25.85	26.00	26.69	26.57	26.25	26.18	26.99	26.19	26.54	26.21	26.83	26.45	26.36	25.72	26.54	26.00	25.66
MnO	2.96	3.17	3.28	2.84	2.86	3.20	3.22	3.22	3.32	2.96	2.96	2.95	3.11	3.04	2.93	3.27	3.10	2.78	3.27
MgO	3.59	3.95	3.91	3.73	3.74	3.79	3.93	4.04	3.99	3.80	3.80	3.99	3.93	3.58	3.70	3.82	3.86	3.71	3.97
CaO	6.46	6.08	6.24	6.36	6.20	6.24	6.36	6.06	6.39	6.75	6.64	6.43	6.43	6.32	6.32	6.41	6.39	6.61	6.53
Total	99.77	100.64	99.45	99.38	100.18	100.04	99.94	99.28	100.45	99.90	100.27	100.34	100.44	99.88	99.36	99.47	100.06	99.32	100.19
Cations on the basis of 12 oxygens																			
Si	3.07	3.03	3.07	3.09	3.08	3.06	3.06	3.04	3.03	3.05	3.05	3.08	3.04	3.08	3.07	3.08	3.06	3.08	3.07
Ti	0.01	0.00	0.01	0.00	0.01	0.01	0.00	0.00	0.00	0.00	0.00	0.00	0.01	0.01	0.00	0.01	0.01	0.01	0.00
Al	2.00	1.99	1.99	2.01	2.00	1.99	1.99	2.00	1.96	2.00	1.99	1.99	1.98	2.00	2.00	1.99	1.98	1.99	2.00
Fe*	1.75	1.80	1.72	1.73	1.76	1.76	1.73	1.74	1.78	1.73	1.75	1.72	1.76	1.75	1.75	1.71	1.75	1.73	1.69
Mn	0.20	0.21	0.22	0.19	0.19	0.21	0.22	0.22	0.22	0.20	0.20	0.20	0.21	0.20	0.20	0.22	0.21	0.19	0.22
Mg	0.42	0.46	0.46	0.44	0.44	0.44	0.46	0.48	0.47	0.45	0.45	0.47	0.46	0.42	0.44	0.45	0.45	0.44	0.47
Ca	0.55	0.51	0.53	0.54	0.52	0.53	0.54	0.52	0.54	0.57	0.56	0.54	0.54	0.54	0.54	0.54	0.54	0.56	0.55
Total	8.00	8.00	8.00	8.00	8.00	8.00	8.00	8.00	8.00	8.00	8.00	8.00	8.00	8.00	8.00	8.00	8.00	8.00	8.00
X_{Prp}	0.14	0.16	0.16	0.15	0.15	0.15	0.16	0.16	0.16	0.15	0.15	0.16	0.16	0.15	0.15	0.15	0.16	0.15	0.16
X_{alm}	0.60	0.60	0.58	0.59	0.60	0.60	0.59	0.60	0.59	0.59	0.59	0.59	0.59	0.60	0.60	0.58	0.59	0.59	0.58
X_{Grs}	0.19	0.17	0.18	0.19	0.18	0.18	0.18	0.17	0.18	0.19	0.19	0.18	0.18	0.18	0.18	0.19	0.18	0.19	0.19
X_{Sps}	0.07	0.07	0.08	0.07	0.07	0.07	0.07	0.07	0.07	0.07	0.07	0.07	0.07	0.07	0.07	0.08	0.07	0.07	0.07

**Total Fe as FeO*

Table 1. (continued)

Sample	2KT9																			
Analysis	133	134	135	136	137	138	139	140	141	143	144	145	146	147	148	154	156	157	158	
Mode	Grt 1	Grt 1	Grt 1	Grt 1	Grt 1	Grt 1	Grt 1	Grt 1	Grt 1	Grt 1	Grt 1	Grt 1	Grt 1	Grt 1	Grt 1	Grt 1	Grt 1	Grt 1	Grt 1	
	Core	→	→	→	→	→	→	→	→	→	→	→	→	→	→	→	→	→	→	→
SiO_2	38.94	38.89	38.88	38.49	38.47	38.74	38.95	39.00	38.67	39.00	38.98	38.69	38.81	38.60	38.93	38.75	38.94	38.98	38.81	
TiO_2	0.08	0.12	0.12	0.09	0.10	0.11	0.13	0.09	0.06	0.04	0.07	0.00	0.02	0.08	0.10	0.05	0.11	0.12	0.02	
Al_2O_3	21.41	21.21	21.25	21.05	21.13	21.32	21.36	21.41	21.50	21.55	21.55	21.56	21.79	21.40	21.53	21.61	21.48	21.41	21.42	
FeO*	25.91	26.37	26.44	26.29	26.12	26.57	25.79	26.53	25.53	26.72	26.30	26.07	25.86	25.44	25.28	26.09	26.40	26.28	25.57	
MnO	3.44	3.26	3.17	3.01	3.00	3.09	3.27	3.18	3.18	3.24	3.01	3.03	3.21	3.30	3.49	3.14	3.17	3.47	3.40	
MgO	4.03	4.04	4.09	3.79	4.00	4.03	3.68	3.89	3.82	3.86	3.79	3.90	3.87	3.94	3.85	3.89	3.80	3.87	3.83	
CaO	6.59	6.52	6.52	6.68	6.58	6.82	6.92	6.69	6.32	6.27	6.31	6.41	6.37	6.33	6.27	6.26	6.49	6.20	6.29	
Total	100.40	100.41	100.47	99.40	99.40	100.68	100.10	100.79	99.08	100.68	100.01	99.66	99.93	99.09	99.45	99.79	100.39	100.33	99.34	
Cations on the basis of 12 oxygens																				
Si	3.06	3.06	3.05	3.06	3.05	3.04	3.07	3.05	3.08	3.06	3.08	3.06	3.06	3.07	3.09	3.06	3.06	3.07	3.08	
Ti	0.01	0.01	0.01	0.00	0.01	0.01	0.01	0.01	0.00	0.00	0.00	0.00	0.00	0.00	0.01	0.00	0.01	0.01	0.00	
Al	1.98	1.96	1.96	1.97	1.98	1.97	1.99	1.98	2.02	1.99	2.00	2.01	2.02	2.01	2.01	2.01	1.99	1.99	2.00	
Fe*	1.70	1.73	1.74	1.75	1.73	1.74	1.70	1.74	1.70	1.75	1.74	1.73	1.71	1.69	1.68	1.73	1.74	1.73	1.70	
Mn	0.23	0.22	0.21	0.20	0.20	0.20	0.22	0.21	0.21	0.22	0.20	0.20	0.21	0.22	0.23	0.21	0.21	0.23	0.23	
Mg	0.47	0.47	0.48	0.45	0.47	0.47	0.43	0.45	0.45	0.45	0.45	0.46	0.46	0.47	0.45	0.46	0.44	0.45	0.45	
Ca	0.55	0.55	0.55	0.57	0.56	0.57	0.58	0.56	0.54	0.53	0.53	0.54	0.54	0.54	0.53	0.53	0.55	0.52	0.54	
Total	8.00	8.00	8.00	7.99	8.00	8.00	8.00	8.00	8.00	8.00	8.00	8.00	8.00	8.00	8.00	8.00	8.00	8.00	8.00	
X_{Prp}	0.16	0.16	0.16	0.15	0.16	0.16	0.15	0.15	0.16	0.15	0.15	0.16	0.16	0.16	0.16	0.16	0.15	0.15	0.16	
X_{alm}	0.56	0.58	0.58	0.59	0.58	0.58	0.58	0.59	0.58	0.60	0.60	0.59	0.59	0.58	0.58	0.59	0.59	0.59	0.58	
X_{Grs}	0.20	0.19	0.19	0.19	0.19	0.19	0.20	0.19	0.19	0.18	0.18	0.18	0.18	0.18	0.18	0.18	0.19	0.18	0.18	
X_{Sps}	0.08	0.07	0.07	0.07	0.07	0.07	0.07	0.07	0.07	0.07	0.07	0.07	0.07	0.08	0.08	0.07	0.07	0.08	0.08	

**Total Fe as FeO*

Sample	2KT9																			
Analysis	159	160	161	162	163	164	165	166	167	169	170	171	173	174	175	176	177	178	179	
Mode	Grt 1	Grt 1	Grt 1	Grt 1	Grt 1	Grt 1	Grt 1	Grt 1	Grt 1	Grt 1	Grt 1	Grt 1	Grt 1	Grt 1	Grt 1	Grt 1	Grt 1	Grt 1	Grt 1	
	→	→	→	→	→	→	→	→	→	→	→	→	→	→	→	→	→	→	→	
SiO_2	38.77	38.72	38.67	38.78	39.16	38.83	38.61	38.35	38.67	39.00	38.95	38.66	38.79	38.69	37.99	38.89	38.94	38.86	38.93	
TiO_2	0.10	0.06	0.10	0.13	0.10	0.09	0.08	0.08	0.11	0.10	0.08	0.09	0.01	0.06	0.08	0.07	0.05	0.09	0.00	
Al_2O_3	21.26	21.25	21.45	21.37	21.36	21.30	21.20	21.22	21.09	21.31	21.33	21.47	21.49	21.30	21.22	21.56	21.47	21.62	21.57	
FeO*	25.94	26.06	26.55	26.49	26.05	26.59	27.55	26.80	26.60	26.13	26.53	25.89	25.82	25.87	26.91	26.46	25.96	26.26	26.50	
MnO	3.33	3.14	3.27	3.29	3.11	3.41	2.97	3.10	3.14	3.02	3.13	3.05	2.82	2.98	3.26	2.64	2.95	2.95	3.03	
MgO	3.90	3.72	3.84	3.87	3.78	4.05	3.73	3.80	3.98	3.84	4.00	3.69	3.75	3.55	3.22	3.76	4.08	4.12	4.08	
CaO	6.23	6.01	6.24	6.32	6.47	6.19	6.21	6.39	6.40	6.51	6.73	6.50	6.36	6.70	6.58	6.28	6.41	6.34	6.23	
Total	99.53	98.96	100.12	100.25	100.03	100.46	100.35	99.74	99.99	99.91	100.75	99.35	99.04	99.15	99.26	99.66	99.86	100.24	100.34	
Cations on the basis of 12 oxygens																				
Si	3.07	3.09	3.05	3.06	3.09	3.05	3.05	3.04	3.05	3.08	3.05	3.07	3.09	3.08	3.03	3.08	3.07	3.05	3.06	
Ti	0.01	0.01	0.01	0.01	0.01	0.01	0.00	0.00	0.01	0.01	0.00	0.00	0.00	0.01	0.01	0.01	0.00	0.01	0.00	
Al	1.99	2.00	1.99	1.98	1.99	1.97	1.97	1.98	1.96	1.98	1.97	2.01	2.02	2.00	2.00	2.01	2.00	2.00	2.00	
Fe*	1.72	1.74	1.75	1.75	1.72	1.75	1.82	1.78	1.76	1.73	1.74	1.72	1.72	1.72	1.80	1.75	1.71	1.73	1.74	
Mn	0.22	0.21	0.22	0.22	0.21	0.23	0.20	0.21	0.21	0.20	0.21	0.21	0.19	0.20	0.22	0.18	0.20	0.20	0.20	
Mg	0.46	0.44	0.45	0.45	0.44	0.47	0.44	0.45	0.47	0.45	0.47	0.44	0.44	0.42	0.38	0.44	0.48	0.48	0.48	
Ca	0.53	0.51	0.53	0.53	0.55	0.52	0.52	0.54	0.54	0.55	0.56	0.55	0.54	0.57	0.56	0.53	0.54	0.53	0.52	
Total	8.00	8.00	8.00	8.00	8.00	8.00	8.00	8.00	8.00	8.00	8.00	8.00	8.00	8.00	8.00	8.00	8.00	8.00	8.00	
X_{Prp}	0.16	0.15	0.15	0.16	0.15	0.16	0.15	0.15	0.16	0.15	0.16	0.15	0.15	0.14	0.13	0.16	0.16	0.16	0.16	
X_{alm}	0.59	0.60	0.59	0.59	0.59	0.59	0.60	0.60	0.59	0.59	0.58	0.59	0.59	0.59	0.61	0.60	0.59	0.59	0.59	
X_{Grs}	0.18	0.18	0.18	0.18	0.19	0.18	0.18	0.18	0.18	0.19	0.19	0.19	0.19	0.20	0.19	0.18	0.18	0.18	0.18	
X_{Sps}	0.07	0.07	0.07	0.07	0.07	0.07	0.07	0.07	0.07	0.07	0.07	0.07	0.07	0.07	0.07	0.06	0.07	0.07	0.07	

**Total Fe as FeO*

Sample	2KT9																			
Analysis	180	181	183	184	185	186	187	188	189	190	195	199	201	202	204	208	210	211	212	
Mode	Grt 1	Grt 1	Grt 1	Grt 1	Grt 1	Grt 1	Grt 1	Grt 1	Grt 1	Grt 1	Grt 1	Grt 1	Grt 1	Grt 1	Grt 1	Grt 1	Grt 1	Grt 1	Grt 1	
	→	→	→	→	→	→	→	→	→	→	→	→	→	→	→	→	→	→	Rim	
SiO_2	39.00	38.79	39.43	39.09	39.15	39.47	39.01	38.51	38.28	38.33	39.24	39.32	39.08	39.26	38.78	38.98	38.78	38.91	38.82	
TiO_2	0.08	0.08	0.07	0.07	0.00	0.10	0.02	0.01	0.11	0.09	0.03	0.10	0.08	0.07	0.05	0.05	0.08	0.11	0.11	
Al_2O_3	21.65	21.60	21.53	21.61	21.74	21.76	21.47	21.53	21.17	20.96	21.51	21.73	21.58	21.60	21.46	21.48	21.58	21.81	21.43	
FeO*	26.19	26.33	25.25	26.42	26.29	26.23	26.92	27.95	27.04	28.15	26.46	25.75	25.96	25.99	26.69	26.57	26.26	26.32	27.28	
MnO	2.99	2.92	1.55	1.37	1.59	1.21	1.01	2.18	2.44	1.89	1.34	1.07	1.16	1.20	1.32	0.87	0.92	0.98	1.16	
MgO	4.08	4.02	4.69	4.93	4.39	5.39	5.50	4.10	3.89	4.43	4.73	5.22	4.80	4.78	4.74	5.32	5.35	5.06	4.52	
CaO	6.20	6.24	6.51	6.11	6.96	6.32	6.16	5.98	6.76	6.45	5.84	5.89	6.33	6.30	6.03	6.03	5.99	6.01	6.23	
Total	100.19	99.98	99.03	99.60	100.12	100.48	100.09	100.26	99.69	100.30	99.15	99.08	98.99	99.20	99.07	99.30	98.96	99.20	99.55	
Cations on the basis of 12 oxygens																				
Si	3.07	3.06	3.12	3.07	3.07	3.07	3.05	3.03	3.03	3.01	3.10	3.10	3.09	3.10	3.07	3.07	3.06	3.07	3.06	
Ti	0.00	0.00	0.01	0.01	0.00	0.01	0.00	0.00	0.01	0.01	0.00	0.00	0.00	0.00	0.00	0.00	0.00	0.01	0.01	
Al	2.01	2.01	2.00	2.00	2.01	1.99	1.97	2.00	1.98	1.94	2.00	2.02	2.01	2.01	2.00	1.99	2.01	2.03	1.99	
Fe*	1.72	1.74	1.67	1.74	1.72	1.70	1.76	1.84	1.79	1.85	1.75	1.70	1.72	1.72	1.77	1.75	1.73	1.73	1.80	
Mn	0.20	0.19	0.10	0.09	0.11	0.08	0.07	0.15	0.16	0.13	0.09	0.07	0.08	0.08	0.09	0.06	0.06	0.06	0.08	
Mg	0.48	0.47	0.55	0.58	0.51	0.62	0.64	0.48	0.46	0.52	0.56	0.61	0.56	0.56	0.56	0.62	0.63	0.59	0.53	
Ca	0.52	0.53	0.55	0.51	0.58	0.53	0.51	0.50	0.57	0.54	0.50	0.50	0.54	0.53	0.51	0.51	0.51	0.51	0.53	
Total	8.00	8.00	8.00	8.00	8.00	8.00	8.00	8.00	8.00	8.00	8.00	8.00	8.00	8.00	8.00	8.00	8.00	8.00	8.00	
X_{Prp}	0.16	0.16	0.19	0.20	0.17	0.21	0.21	0.16	0.16	0.17	0.19	0.21	0.20	0.19	0.19	0.21	0.22	0.21	0.18	
X_{alm}	0.59	0.59	0.58	0.59	0.59	0.58	0.59	0.62	0.60	0.61	0.61	0.59	0.59	0.59	0.61	0.59	0.59	0.60	0.61	
X_{Grs}	0.18	0.18	0.19	0.18	0.20	0.18	0.18	0.17	0.19	0.18	0.17	0.17	0.18	0.19	0.17	0.18	0.17	0.17	0.18	
X_{Sps}	0.07	0.07	0.04	0.03	0.04	0.03	0.02	0.05	0.05	0.04	0.03	0.03	0.03	0.03	0.03	0.02	0.02	0.02	0.03	

**Total Fe as FeO*

Table 1. (continued)

Sample	2KT9																		
Analysis	93	96	97	98	99	100	101	102	2	3	4	5	6	7	8	9	10	11	12
Mode	Grt 1	Grt 1	Grt 1	Grt 1	Grt 1	Grt 1	Grt 1	Grt 1	Grt 2	Grt 2	Grt 2	Grt 2	Grt 2	Grt 2	Grt 2	Grt 2	Grt 2	Grt 2	Grt 2
	Rim	→	→	→	→	→	→	Rim	Rim	←	←	←	←	←	←	←	←	Core	←
SiO_2	37.38	37.14	37.43	37.55	37.35	38.44	38.27	38.35	38.32	38.66	39.06	38.94	38.69	38.60	38.51	39.66	38.23	38.63	38.97
TiO_2	0.12	0.04	0.03	0.03	0.02	0.04	0.10	0.03	0.00	0.06	0.06	0.02	0.04	0.05	0.05	0.03	0.12	0.06	0.07
Al_2O_3	20.88	20.90	21.00	21.51	21.28	21.57	21.83	21.70	21.16	21.23	21.02	21.27	20.99	21.19	21.17	20.51	21.12	20.85	20.79
FeO*	26.26	27.40	27.41	27.35	26.35	23.13	23.31	23.52	28.66	28.95	28.41	28.37	28.35	28.46	28.98	28.43	28.67	28.70	28.81
MnO	1.95	2.56	2.45	2.52	1.73	0.67	0.68	0.65	2.83	1.25	1.36	1.39	1.41	1.34	1.49	1.46	1.60	1.62	1.82
MgO	5.18	4.14	4.19	4.11	4.69	5.45	5.48	5.56	3.93	4.83	4.72	4.76	4.77	4.68	4.58	4.81	4.54	4.50	4.42
CaO	7.14	6.75	7.21	6.96	8.02	10.80	10.58	10.43	5.67	5.95	5.93	5.90	5.96	5.97	6.11	5.86	5.86	6.11	6.08
Total	98.91	98.93	99.72	100.03	99.44	100.10	100.25	100.24	100.57	100.93	100.56	100.65	100.21	100.29	100.89	100.76	100.14	100.47	100.96
Cations on the basis of 12 oxygens																			
Si	2.96	2.96	2.96	2.96	2.94	2.97	2.95	2.96	3.02	3.02	3.06	3.05	3.04	3.03	3.01	3.10	3.01	3.03	3.05
Ti	0.01	0.00	0.00	0.00	0.00	0.00	0.01	0.00	0.00	0.00	0.01	0.00	0.00	0.00	0.00	0.00	0.01	0.00	0.01
Al	1.95	1.97	1.96	2.00	1.98	1.97	1.99	1.98	1.96	1.95	1.95	1.96	1.95	1.96	1.95	1.89	1.96	1.93	1.92
Fe*	1.74	1.83	1.81	1.80	1.74	1.50	1.50	1.52	1.89	1.89	1.86	1.86	1.86	1.87	1.89	1.86	1.89	1.89	1.89
Mn	0.13	0.17	0.16	0.17	0.11	0.04	0.05	0.04	0.19	0.08	0.09	0.09	0.09	0.09	0.10	0.10	0.11	0.11	0.12
Mg	0.61	0.49	0.50	0.48	0.55	0.63	0.63	0.64	0.46	0.56	0.55	0.55	0.56	0.55	0.53	0.56	0.53	0.53	0.52
Ca	0.60	0.58	0.61	0.59	0.68	0.89	0.87	0.86	0.48	0.50	0.50	0.49	0.50	0.50	0.51	0.49	0.49	0.51	0.51
Total	8.00	8.00	8.00	8.00	8.00	8.00	8.00	8.00	8.00	8.00	8.00	8.00	8.00	8.00	8.00	8.00	8.00	8.00	8.00
X_{Prp}	0.21	0.17	0.17	0.16	0.19	0.21	0.21	0.22	0.15	0.19	0.18	0.18	0.18	0.18	0.18	0.19	0.18	0.17	0.17
X_{alm}	0.55	0.58	0.57	0.58	0.54	0.47	0.48	0.48	0.63	0.62	0.62	0.62	0.62	0.62	0.62	0.62	0.62	0.62	0.62
X_{Grs}	0.20	0.19	0.20	0.20	0.23	0.30	0.30	0.29	0.16	0.16	0.17	0.17	0.17	0.17	0.17	0.16	0.16	0.17	0.17
X_{Sps}	0.04	0.06	0.06	0.06	0.04	0.02	0.01	0.01	0.06	0.03	0.03	0.03	0.03	0.03	0.03	0.03	0.04	0.04	0.04

**Total Fe as FeO*

Sample	2KT9					
Analysis	13	14	15	16	17	18
Mode	Grt 2	Grt 2	Grt 2	Grt 2	Grt 2	Grt 2
	←	←	←	←	←	Rim
SiO_2	38.77	38.60	38.74	38.77	38.53	38.45
TiO_2	0.09	0.05	0.08	0.06	0.04	0.06
Al_2O_3	20.77	20.99	21.12	21.21	21.25	21.02
FeO*	28.41	28.52	28.27	28.73	28.24	28.17
MnO	1.74	1.62	1.62	1.26	2.82	2.66
MgO	4.30	4.67	4.67	4.90	4.09	4.07
CaO	6.31	6.17	6.30	6.06	5.86	5.60
Total	100.39	100.62	100.80	100.99	100.83	100.03
Cations on the basis of 12 oxygens						
Si	3.05	3.02	3.03	3.02	3.02	3.04
Ti	0.00	0.00	0.00	0.00	0.00	0.00
Al	1.93	1.94	1.94	1.95	1.97	1.96
Fe*	1.87	1.87	1.85	1.87	1.85	1.86
Mn	0.12	0.11	0.11	0.08	0.19	0.18
Mg	0.50	0.54	0.54	0.57	0.48	0.48
Ca	0.53	0.52	0.53	0.50	0.49	0.48
Total	8.00	8.00	8.00	8.00	8.00	8.00
X_{Prp}	0.17	0.18	0.18	0.19	0.16	0.16
X_{alm}	0.62	0.61	0.61	0.62	0.62	0.62
X_{Grs}	0.17	0.17	0.17	0.16	0.16	0.16
X_{Sps}	0.04	0.04	0.04	0.03	0.06	0.06

**Total Fe as FeO*